# THE IMPORTANT ROLE OF ANTENNA PATTERN CHARACTERIZATION IN THE ABSOLUTE CALIBRATION OF GNSS-R MEASUREMENTS

*Tianlin Wang[1], Christopher Ruf[1], Andrew O'Brien[2], Scott Gleason[3], Darren McKague[1], Anthony Russel[1]*

[1]University of Michigan, Ann Arbor, MI USA
[2]The Ohio State University, Columbus, OH USA
[3]University Corporation for Atmospheric Research, Boulder, CO USA

## ABSTRACT

The v3 CYGNSS Level 1 calibration algorithm uses the direct signal received by the navigation channel to estimate the GPS EIRP for calibration of the NBRCS. Three sets of antenna patterns play an important role in this calibration algorithm, including the GPS transmit antenna and the CYGNSS zenith and nadir receive antennas. In this paper, we examine how the three antenna patterns are characterized on-orbit and how they are used by the CYGNSS Level 1b calibration algorithm. The impact of antenna pattern knowledge on calibration uncertainty is evaluated and discussed.

***Index Terms***— Antenna pattern, calibration, CYGNSS, GNSS-R, GPS, spaceborne measurement, remote sensing

## 1. INTRODUCTION

GNSS-Reflectometry (GNSS-R) uses the reflected GNSS signals from the Earth surface for remote sensing applications. The primary GNSS-R observable is the Delay Doppler Map (DDM). The intensity of every DDM pixel is proportional to the scattered power originating from the surface [1], [2]. A general calibration procedure for GNSS-R measurements is to derive the bistatic radar cross section (BRCS) from the raw measurements of received power and then normalize them by the scattering area to obtain normalized BRCS.

NASA's Cyclone Navigation Satellite System (CYGNSS) Earth Venture mission uses the Global Positioning System (GPS) as an active source [3], [4]. Its calibration includes: Level 1a calibration converts each bin in the Level 0 DDM from raw counts to units of watts, and Level 1b calibrates the power into the normalized BRCS (NBRCS) [5], [6].

One key parameter used in the calibration of NRBCS is the effective isotropic radiated power (EIRP) of the Global Navigation System (GPS) satellites, defined as the product of transmit power and antenna gain. To address the uncertainties existing in EIRP estimate, a dynamic calibration approach is developed to use the direct received GPS signal to estimate GPS EIRP in the specular reflected direction and then incorporates it into the calibration of NBRCS [7], [8], as shown in Fig. 1. To use the direct signal, accurate knowledge of both the CYGNSS zenith receive antenna pattern and the GPS transmit antenna pattern are required.

Another important parameter is the gain pattern of the CYGNSS nadir receive antenna. The pattern was estimated measured prior to launch. However, on-orbit measurements indicate that the satellite bus (e.g. solar panels) have a significant impact on its pattern. This suggests that the pattern should be characterized on-orbit measurements.

To summarize, there are three sets of antenna patterns used in the calibration algorithm. The CYGNSS zenith antenna and GPS transmit antenna are used to estimate the GPS EIRP and the CYGNSS nadir antenna, used to receive scattered GPS signals from the Earth surface, is used to determine the NBRCS. In this paper, we will investigate detailed characterization of these antenna patterns and their implementation in the CYGNSS L1b calibration algorithm. The performance improvement will also be evaluated.

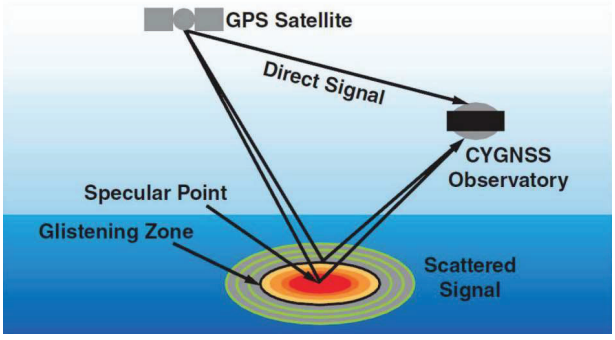


**Fig. 1** The conceptual diagram of CYGNSS calibration algorithm

## 2. ROLE OF ANTENNA PATTENS IN CYGNSS LEVEL 1 CALIBRATION

The CYGNSS L1b calibration generates two data products associated with each L1a DDM: 1) a bin-by-bin calculation

of the surface BRCS, or σ, and 2) bin-by-bin values of the effective scattering areas. With other metadata, these two intermediate variables are used to compute the NBRCS [5] as

$$\bar{\sigma}(\hat{\tau},\hat{f}) = \frac{P_g(\hat{\tau},\hat{f})(4\pi)^3}{E_S \lambda^2 G_S^R R_S^{Total}} \quad (1)$$

where $P_g(\hat{\tau},\hat{f})$ is the Level 1a calibrated signal power at a specific delay ($\hat{\tau}$) and Doppler ($\hat{f}$) bin, $E_S$ is the GPS EIRP in the direction of the specular reflection point, $\lambda$ is the wavelength for GPS L1 signals, $G_S^R$ is the receiver antenna gain at the specular point, and $R_S^{Total}$ is the total range loss from the transmitter to the surface plus the surface to the receiver at the specular point.

The estimated GPS satellite EIRP in the specular point direction is calculated as

$$E_S = \frac{(4\pi R)^2}{\lambda^2} \frac{P_Z}{G_{LNA}(T_{LNA}) G_R(\theta_R,\phi_R) \widehat{ZSR}(\theta_{inc})} \quad (2)$$

where $R$ is the distance between the GPS transmitter and the zenith receiver, $\lambda$ is the wavelength for GPS L1 signals, $P_z$ is the converted zenith power at the DMR input port, $G_{LNA}$ is the zenith LNA gain, $G_R$ is the zenith antenna gain, and $ZSR$ is the zenith-to-specular function. The estimated EIRP is used in the CYGNSS L1b calibration algorithm to estimate NBRCS from the CYGNSS measurements.

For the dynamic EIRP calibration of GPS EIRP, the two key parameter is the zenith receiver antenna gain $G_R$ and the zenith-to-specular ratio (ZSR) function. The ZSR function is derived from the GPS antenna gain pattern.

## 3. CALIBRATION TECHNIQUE FOR THE ANTENNA GAIN PATTERNS

Gain patterns of the GPS transmit antenna and CYGNSS zenith antenna are estimated using the spaceborne antenna range measurement system formed by the GPS and CYGNSS constellations, as shown in Fig. 2. Actual on-orbit data are used to determine the two sets of patterns in their operational environment. A high-resolution map of the complete on-Earth portion of the GPS antenna's main beam results. A robustness test suggests that the procedure converges to a final set of patterns that is independent of first guess assumptions about the patterns [9] [10].

For the nadir antenna gain pattern, an empirical correction was previously derived by using anomalies in the NBRCS observations [6]. A subsequent approach was developed to correct the antenna pattern using intercomparisons of measured and modeled NBRCS, where the modeled NBRCS is derived from modeled mean squared slope (MSS), which is developed by adding the contribution of a high frequency tail to the IFREMER WAVEWATCH III (WW3) MSS [11]. Collaboration with the CYGNSS wave-model working group provides us 1) alternate approach using other wave models [12], [13] and in-situ buoy observations; 2) selection algorithm of the MSS subsets that are optimal for the calibration of nadir science antenna patterns.

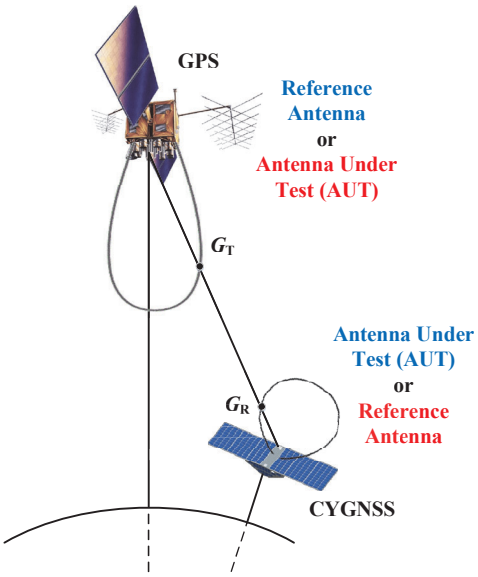


**Fig. 2** Spaceborne antenna range measurement system formed by constellations of GPS and CYGNSS satellites

## 4. SUMMARY

This work will provide an update of the characterization of the antenna gain patterns used for the v3.1 CYGNSS L1b calibration algorithm, including the GPS transmit antenna, and the zenith and nadir receive antennas of the CYGNSS satellites. The impact on the quality of calibration will also be discussed during the IGARSS presentation.

## 5. REFERENCES

[1] V. U. Zavorotny and A. G. Voronovich, "Scattering of GPS signals from the ocean with wind remote sensing application," *IEEE Transactions on Geoscience and Remote Sensing*, vol. 38, no. 2, pp. 951-964, March 2000, doi: 10.1109/36.841977.

[2] V. U. Zavorotny, S. Gleason, E. Cardellach, and A. Camps, "Tutorial on remote sensing using GNSS bistatic radar of opportunity," *IEEE Geoscience and Remote Sensing Magazine*, vol. 2, no. 4, pp. 8-45, Dec. 2014, doi: 10.1109/MGRS.2014.2374220.

[3] C. S. Ruf, S. Gleason, Z. Jelenak, S. Katzberg, A. Ridley, R. Rose, J. Scherrer, and V. Zavorotny, "The CYGNSS nanosatellite constellation hurricane mission," 2012 IEEE International Geoscience and Remote Sensing Symposium, Munich, 2012, pp. 214-216, doi: 10.1109/IGARSS.2012.6351600.

[4] M. Unwin, J. Dickinson, R. Rose, D. Rose, M. Vincent, and A. Lyons, "CYGNSS: Enabling the Future of Hurricane Prediction

[Remote Sensing Satellites]," *IEEE Geoscience and Remote Sensing Magazine*, vol. 1, no. 2, pp. 52-67, June 2013, doi: 10.1109/MGRS.2013.2260911.

[5] S. Gleason, C. S. Ruf, M. P. Clarizia, and A. J. O'Brien, "Calibration and Unwrapping of the Normalized Scattering Cross Section for the Cyclone Global Navigation Satellite System," *IEEE Transactions on Geoscience and Remote Sensing*, vol. 54, no. 5, pp. 2495-2509, May 2016, doi: 10.1109/TGRS.2015.2502245.

[6] S. Gleason, C. S. Ruf, A. J. Orbrien, and D. S. McKague, "The CYGNSS Level 1 Calibration Algorithm and Error Analysis Based on On-Orbit Measurements," *IEEE Journal of Selected Topics in Applied Earth Observations and Remote Sensing*, vol. 12, no. 1, pp. 37-49, Jan. 2019, doi: 10.1109/JSTARS.2018.2832981.

[7] T. Wang, C. Ruf, S. Gleason, B. Block, D. McKague, and A. O'Brien, "A Real-Time EIRP Level 1 Calibration Algorithm for the CYGNSS Mission Using the Zenith Measurements," 2019 IEEE International Geoscience and Remote Sensing Symposium, Yokohama, pp. 8725-8728, doi: 10.1109/IGARSS.2019.8900456.

[8] T. Wang, C. Ruf, S. Gleason, A. O'Brien, D. McKague, B. Block, and A. Russel, "Dynamic Calibration of GPS Effective Isotropic Radiated Power for GNSS-Reflectometry Earth Remote Sensing," submitted to *IEEE Transactions on Geoscience and Remote Sensing*, under review.

[9] T. Wang, C. Ruf, A. O'Brien, S. Gleason, D. McKague, B. Block, and A. Russel, "Measurement of GPS and CYGNSS Antenna Gain Patterns with a Spaceborne Antenna Range," submitted to *IEEE Transactions on Antennas and Propagation*, under review.

[10] T. Wang and C. Ruf, "Measuring GPS EIRP in Real-Time with a Spaceborne GNSS-Reflectometry Remote Sensing System," 2021 National Radio Science Meeting (NRSM), Virtual Conference.

[11] T. Wang, V. U. Zavorotny, J. Johnson, Y. Yi, C. Ruf, S. Gleason, D. McKague, P. Hwang, E. Rogers, S. Chen, Y. Pan, and T. Bakker, "Improvement of CYGNSS Level 1 Calibration Using Modeling and Measurements of Ocean Surface Mean Square Slope," 2020 IEEE International Geoscience and Remote Sensing Symposium, Virtual Conference.

[12] P. A. Hwang, F. J. Ocampo-Torres, and H. García-Nava, "Wind Sea and Swell Separation of 1D Wave Spectrum by a Spectrum Integration Method," *Journal of Atmospheric and Oceanic Technology*, vol. 29, no. 1, pp. 116-128, Jan 2012, doi: 10.1175/JTECH-D-11-00075.1.

[13] S. S. Chen, W. Zhao, M. A. Donelan, and H. L. Tolman, "Directional Wind-Wave Coupling in Fully Coupled Atmosphere-Wave-Ocean Models: Results from CBLAST-hurricane," *Journal of the Atmospheric Sciences*, vol. 70, no. 10, pp. 3198-3215, 2013, doi: 10.1175/JAS-D-12-0157.1.